Tensile Deformation and Fracture Behaviour of Magnesium Matrix Composites Produced by Different Casting Methods

[1]M. Y. Ahmad, [1]P. B. Prangnell and [2]H. Karimzadeh

[1]Manchester Materials Science Centre
UMIST/University of Manchester
Grosvenor Street, Manchester M1 7HS, England
[2]Magnesium Elektron
PO Box 23, Swinton
Manchester M27 8DD, England

SUMMARY: Measurements are reported of the strength, ductility, and elastic behaviour of a magnesium AS41 alloy matrix composite reinforced with SiC particles and produced by different casting methods. Particular emphasis is paid to investigating the effects of different spatial distributions of the reinforcing particles on the composite's mechanical behaviour. The homogeneity of the particle distributions (severity of clustering) was quantified from analysis of the near neighbour inter-particle spacings. The effect of the degree of inhomogeneity of the reinforcement's distribution on the fracture and micro-yielding behaviour of the composites was studied by measuring the particle density along the fracture line, and analysing the derivatives of the material's initial stress-strain responses.

KEYWORDS*:* magnesium matrix composite, SiC particles, tensile properties, fracture, particle distribution, clustering.

INTRODUCTION

Particle reinforced metal matrix composites (MMCs) exhibit some attractive physical and mechanical properties; such as, a low density and coefficient of thermal expansion (CTE), increased stiffness, good thermal conductivity, and high tensile strength. However, their low ductility and poor fracture behaviour have limited the widespread application of these materials [1,2].

The yield and tensile strengths of a MMC are affected by several complex and interrelated factors including, the effect of the matrix alloy, and the reinforcement content, type, and alignment [3,4]. Theoretically additions of a stiff reinforcing phase should increase the elastic modulus of a metal matrix. Unfortunately in particle reinforced composites this improvement is not always readily observable because the reinforcement can give rise to plastic flow in the matrix at low applied stresses [3,5]. These difficulties are partly due to the presence of thermal residual stresses arising from differences in the coefficient of thermal expansion between the matrix and ceramic particles. Within the matrix the thermal stresses are normally in tension, which encourage early matrix plastic flow on tensile loading [6]. The other contributing factor is the inhomogeneity of matrix stress state and, in the vicinity of the angular shaped corners of the reinforcement, highly stressed local regions of the matrix

surpass the flow stress on loading much earlier than the matrix as a whole . In a tensile test the associated microplasticity causes a premature departure from the linear elastic line and this behaviour has been studied in aluminium matrix MMCs by Prangnell et al. [5,7] who used derivatives of the initial stress-strain curve to interpret how the plastic deformation first develops from the onset of local flow in an MMC. The situation is further complicated if the reinforcement distribution is inhomogeneous, as this can lead to higher local stress amplification in clustered regions [8]. This can substantially influence the elastic-plastic behaviour of the material, especially at low strains. The inhomogeneous development of plasticity in the matrix means that the stress-strain curves for particulate reinforced MMCs do not usually exhibit the classical linear-elastic response followed by a defined yield point, which makes the measurement of a tensile elastic modulus and yield point problematic. To counter these difficulties, several alternative methods have been proposed for the measurement of an MMC's stiffness and yielding behaviour [1,5].

In MMCs it is therefore important to minimise inhomogeneity in the reinforcement distribution, during initial processing, to achieve optimum properties [9]. The distribution of particles in cast MMCs produced by molten metal mixing routes usually results in particle clusters and particle free regions on the scale of the solidification structure [10,11]. To date most methods for quantification of the particle distributions in MMCs make use of tessellation based techniques [12,13,14]. Tessellation can be used to define the distance between neighbouring particles with a common cell edge. Analysis of the near-neighbour distances has proved useful in the characterisation of a clustered dispersion [11,14] and has lead to the proposal by Murphy et al. [14] of defining the inhomogeneity of a reinforcement distribution in terms of "clustering parameters", based on the variance, or skewness, of the distribution of the inter-particle spacings.

In this study the relationship between the spatial distribution of the reinforcement and the properties of a magnesium alloy reinforced with SiC particles has been investigated for composite materials produced by a range of casting techniques. The effect of the casting process on the degree of inhomogeneity of the reinforcement's distribution, and the consequent fracture and micro-yielding behaviour of the composites, was studied by measuring the particle density along the fracture line and analysing the derivatives of the materials initial stress-strain responses, respectively. These results have been compared to measurements made of the homogeneity of the particle distributions in the bulk castings (severity of clustering) using near neighbour distances and the clustering parameters proposed by Murphy et al [14].

EXPERIMENTAL PROCEDURES

Materials

Castings of an unreinforced and reinforced magnesium, AS41, alloy were produced by Magnesium Elektron (MEL) using a proprietary melt-stirring process. The reinforcement used was F500-SiC particles with an average size of 10 μm and aspect ratio between 1 and 4, and had a nominal volume fraction of 0.1. Samples of the composite were chill cast and sand cast, into 25 mm diameter bars 100 mm long, and high pressure die cast (HPDC) into 2.5 mm thick component. The chemical composition of the AS41 alloy was; Al - 4.09%, Si - 0.78%, Mn - 0.27%, Fe - 0.003% and balance Mg.

Tensile Testing

The tensile properties were measured at room temperature, 100, 150 and 200 °C, using an Instron tensile testing machine. Because of the geometries of the castings, round 6 mm diameter tensile bars were machined from the sand and chill castings bars, whereas flat plate samples were made from the die castings with the same gauge length, but 2 x 10 mm in cross-section. Three specimens were used for each test temperature. A knife edge extensometer (of

25 mm gauge length) was used to measure the strain. The cross head speed of the tensile testing machine used was 0.5 mm/min. A computerised data logger collected the load and displacement data. To measure the yielding behaviour and elastic moduli, analysis of the stress-strain data was carried out from derivatives of the true stress-true strain curves after the data had been smoothed, according to procedures explained elsewhere [5,7].

Metallographic and Fractography Examinations

The microstructures and fracture surfaces of the broken tensile specimens were examined by optical microscopy and in the SEM. An image analyser (MAGIC SCAN) was used to study the particle morphology and distribution in the structure and to measure the grain sizes of the cast samples. Distributions of inter-particle spacings were determined on a plane section, using the image analyser, by measuring the distances between the centroids of nearest neighbour particles at a magnification of 500 times. For each field of measurement about 40-50 particles were measured and 40-50 fields were analysed for each composite. Metallographic examinations were also carried out on cross-sections of the fracture surfaces. The particle density on the fracture surface was characterised using the ratio (P/F) of the total particle length along the fracture line, over the total fracture line length. The fractured particles was also counted within one particle diameter of the fracture surface and the local volume fraction in the vicinity of the fracture surface was measured from one field of view width below the surface (= 200 μm).

RESULT AND DISCUSSION

Microstructures of the Cast Composites

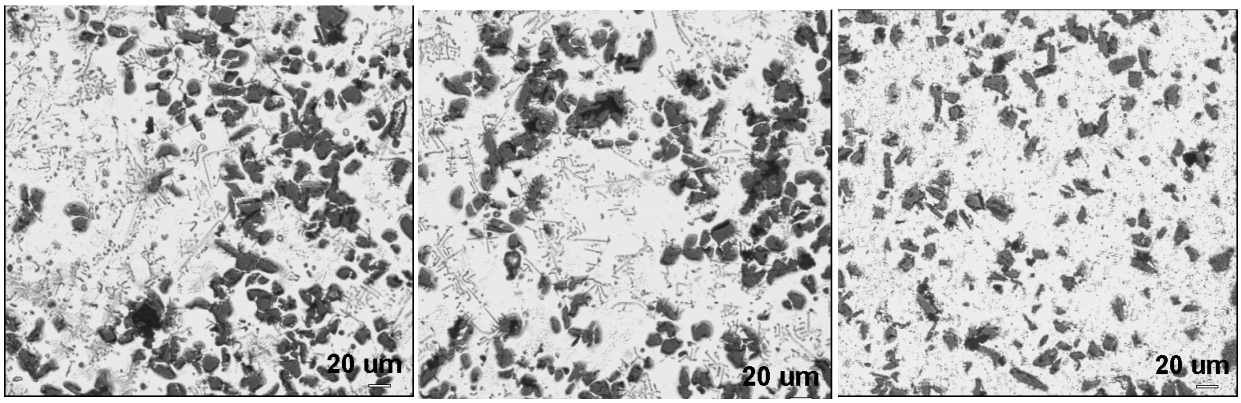

(a) (b) (c)

Fig. 1: Micrographs of the (a) chill cast, (b) sand cast and (c) HPDC AS41 composites.

Figure 1 shows the microstructures of the chill cast, sand and die cast AS41 matrix composites. In figure 1 it can be seen that the distribution of SiC particles in the chill and sand cast composites is not homogeneous. Agglomeration and clustering of the reinforcing particles can be observed throughout the microstructure within the inter-dendritic regions and at the grain boundaries. Other casting defects like pores and non-wetted clusters were also occasionally observed in the regions of high local particle volume fraction. Despite the lower cooling rate, the particle distribution in the sand cast composite appeared less severely segregated than in the chill cast composite. Although there was still pronounced clustering of the reinforcement in the sand cast bars, the particles were not concentrated in as well defined cell boundaries as was seen in the chill cast material. In comparison the die cast composite has a good homogeneous particle distribution and contained few defects. These observations were later confirmed by quantitative analysis of the spatial distribution of the particles (see below) and could be explained by the nature of the casting processes and the cooling rates

during solidification. At the lowest cooling rate, found in the sand cast material, the dendrite arm spacing was much greater than the particle size and the particles were pushed to the interdendritic regions during freezing, together with the solute. In the chill cast material the same effect occurred, but because of the higher cooling rate and smaller dendrite arm spacing the particles were concentrated in thinner layers and tended to be more associated with the grain boundaries. In the pressure die casting, the grains did not develop dendrite arms and the grain size (about 8 μm) was actually finer than the particle size, resulting in a relatively homogeneous random particle distribution. From carrying out castings in wedge shaped copper chill moulds, it was shown that the very small grain size produced in the pressure die castings could not be simply attributed to the higher cooling rate, but was largely as a result of enhanced grain refinement caused by dendrite fragmentation during the die casting process.

In terms of the metallurgical aspects of the microstructure, SEM analysis showed that besides the solid solution of the matrix and SiC particles there were also second phase eutectic Mg_2Si and $Mg_{17}Al_{12}$ precipitates present in the cast structure. The Mg_2Si had the eutectic morphology known as 'Chinese script' and, along with the $Mg_{17}Al_{12}$, was always located along the dendrite and grain boundaries, where the reinforcing particles were also concentrated. These precipitates appeared to have lower volume fraction and were finer in the die cast materials compared to the chill and sand cast composites.

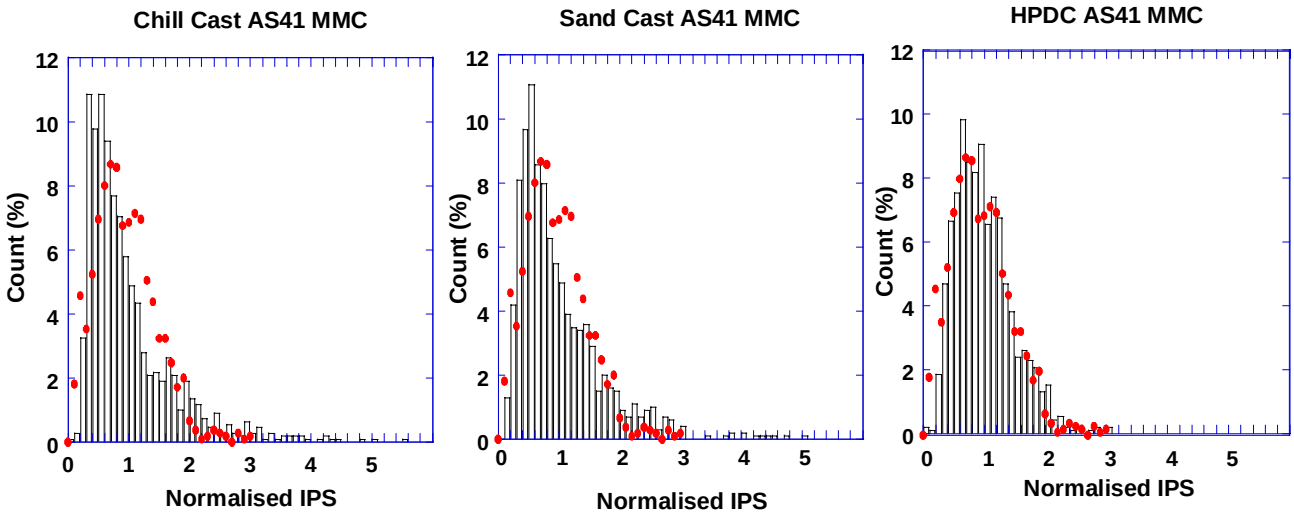

Fig. 2: Histograms of the distribution of normalised inter-particle spacing (IPS) in the high pressure die cast, sand cast and chill cast composite. The distribution obtained from a random set of points is also shown for comparison (●).

Quantification of the Particle Homogeneity

Measurements of inter-particle spacings between near-neighbour particle centeroids was carried out using image analysis. Polygonal cells were constructed from the perpendicular bisectors of lines that connect the centroid of an enclosed particle with those of the surrounding particles. The nearest neighbours of each particle were then defined as the surrounding particles that shared polygon cell edges with the particle of interest. Figure 2 shows the distributions of measured inter-particle spacings in the chill, sand cast and high pressure die cast composites, normalised with respect to the average of the distribution. A distribution of the inter-particle spacings measured in the same way from a similar number of random points, generated by a computer, is also shown in each plot for comparison.

From the histograms, it can be seen that the distribution of particles in the chill and sand cast composites deviates strongly from a random distribution. Their distributions show significant tails, where there are large inter-particle distances in the particle depleted regions of the grain and dendrite arm cores, and peaks in the distributions at values less than that for the random

distribution, indicating particle rich regions. In contrast the inter-particle spacing distribution in the die cast composite appears to be very close to a true random distribution with only a slight deviation from the computer generated data. A small difference can be seen between the interparticle spacing distributions of the chill and sand cast composites. In the chill cast composite the peak in the distribution, at small inter-particle spacings, is slightly less spread.

In order to characterise the particle distributions, in terms of the clustering parameters P1 and P2, the values of variance and skewness for the measured distributions were normalised with respect to those of the ideal random distribution, according to the method suggested by Murphy [14] (defined in table 1). Table 1 shows the values of these parameters. Both clustering parameters, P1 and P2, reflect well the different inhomogeneity of the particle distributions seen in the materials cast by the three alternative processes. For example, the P1 value for HPDC composite is 0.91 (near unity), indicating an almost random distribution, while the P1 values for the sand cast and chill cast composites are above unity (1.97 and 2.19 respectively) which indicates clustered distributions, and shows that the clustering is more pronounced in the chill cast material where particles were concentrated mainly at the grain boundaries. This approach is clearly extremely useful for defining the departure from randomness of the particle distribution in an MMC, but is not sufficient for quantitatively predicting a composites fracture behaviour as it only considers nearest neighbour spacings and does not take into account the interconnectivity of the clusters, or the long range distribution of the higher volume fraction regions.

Table 1: Statistical data for the normalised inter-particle spacing distributions.

Statistical Parameter	High Pressure Die Cast	Sand Cast	Chill Cast	Random Points
Variance, $V= 1/n\Sigma(x- \bar{x})^2$	0.2271	0.4899	0.5450	0.2489
Skewness, $S=\frac{1/n\Sigma(x- \bar{x})^3}{V^{3/2}}$	0.8921	1.8564	2.0498	0.7379
Clustering Parameter, $P1 = V/V_{ran}$	0.9122	1.9677	2.1891	1
Clustering Parameter, $P2 = S/S_{ran}$	1.2089	2.5158	2.7779	1

Tensile Properties

Figure 3 shows typical true stress-strain curves obtained from tensile tests measured at room temperature on the high-pressure die, sand, and chill cast samples of the AS41 alloy reinforced with SiC particles. It can be seen that, despite similar reinforcement volume fractions, the initial loading curves for the sand and chill cast AS41 composites rapidly fall below that of the HPDC composite. The proof stress and ultimate tensile strength for the high-pressure die cast material is also higher than for the sand and chill cast composites. Furthermore, with the sand cast and chill cast composites there is no obvious linear portion of the initial loading curve making measurement of their elastic moduli problematic.

Figure 4 shows the tensile properties of the high pressure die, sand and chill cast, composites as a function of temperature. From figure 4b and c it can be seen that as the temperature increases, the proof stresses and ultimate tensile strengths for all the composites decrease. An

average of three samples was taken for each of the measurements. Nevertheless the elastic moduli for the composites, computed by an Instron data acquisition system, showed considerable scatter in the data and tend to give values for the sand and chill cast materials

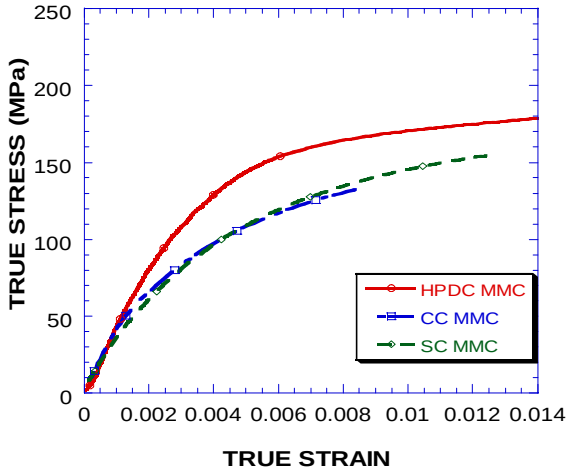

Fig. 3: Typical true stress-strain curves of the high pressure die cast (HPDC), sand cast (SC)and chill cast (CC) composites at room temperature

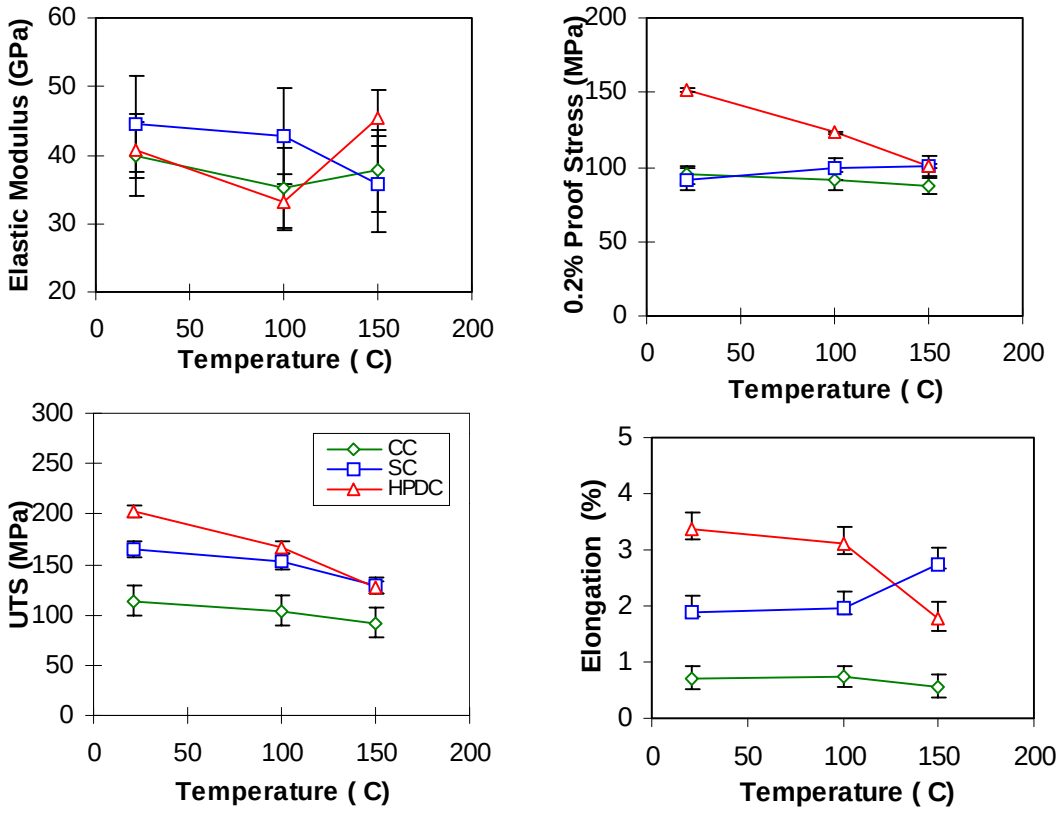

Fig. 4: Tensile properties of the high pressure die cast (HPDC), sand cast (SC) and chill cast (CC) composites as a function of temperature.

that are less than that of the reported value for the matrix alloy (E = 45 GPa). The change in elongation to failure with temperature did not show the trend expected, in that except for the sand cast material it decreased with higher temperature, and this probably reflects the large scatter in the fracture behaviour due to the inhomogeneity of the materials. The generally low stiffness values of the composites suggests a problem in measuring the elastic loading behaviour in tensile tests using conventional methods.

The overall tensile properties of the die cast AS41 composite were considerably better than the those of the other materials and the properties of the sand cast material where slightly better than those of the chill cast composite. This can be explained in terms of the

microstructure, where the distribution of particles in the matrix plays a significant role in determining the properties of the cast composites. Interestingly all the material's properties are ranked in order of the degree of clustering determined by the parameters P1 and P2. The pronounced agglomeration of particles in the chill cast and, to a slightly lesser extent, in the sand cast material has clearly greatly reduced their mechanical properties. It is, however, difficult to entirely separate the effect of differences in the reinforcement particle distributions from those due to changes in the second phase intermetallic particles and the solute levels in solution in the matrix, which would also be affected by the different casting processes.

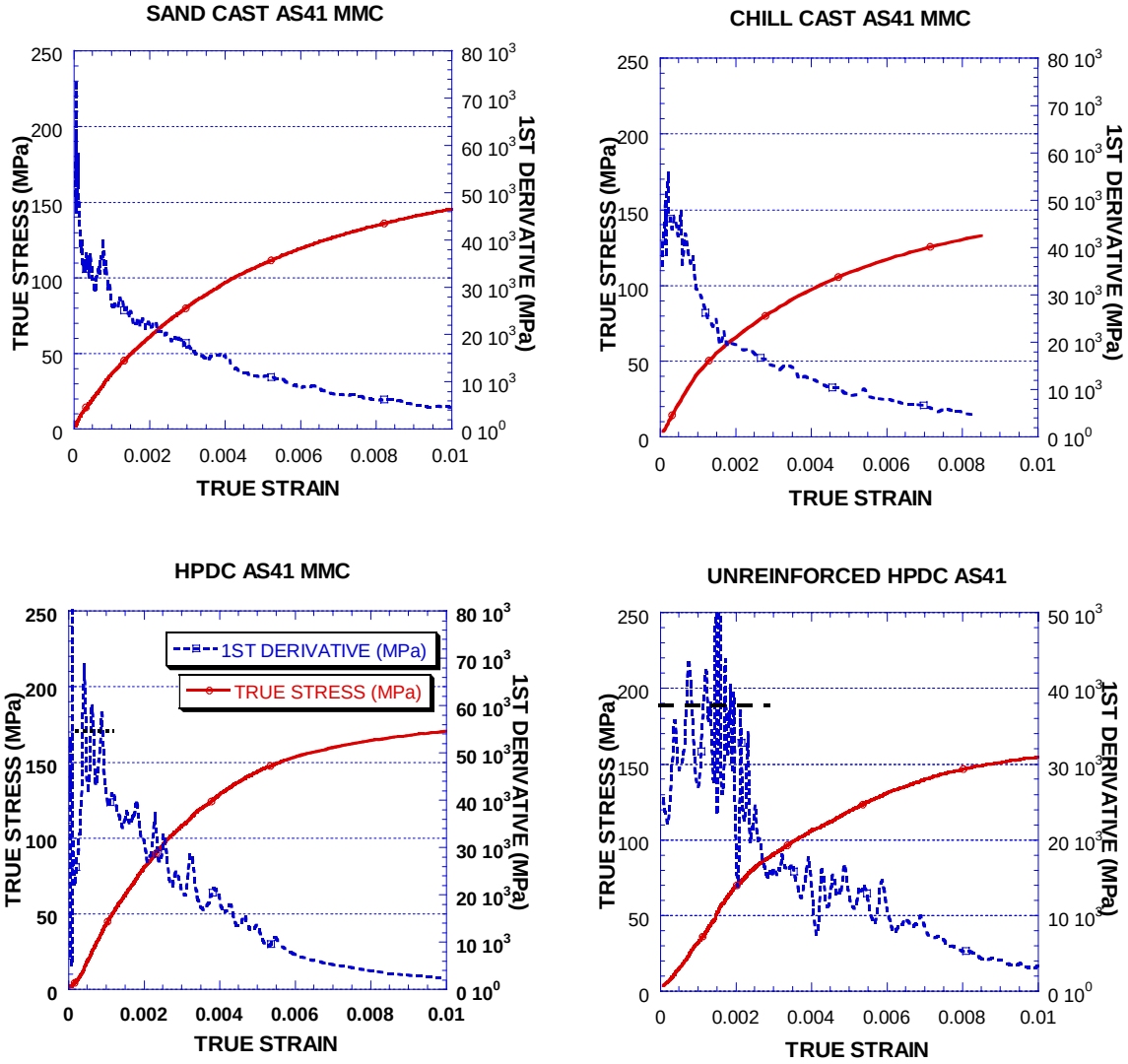

Figure 5 The stress-strain and 1st derivative curves of the HPDC, sand cast and chill cast AS41 composites. The corresponding curves for the unreinforced HPDC AS41 alloy are also shown for comparison. Note the plateau at the initial strain (horizontal dotted lines).

Analysis of the Stress-Strain Curves

Figure 5 shows the local slopes of the of the stress-strain curves (the first derivative ($d\sigma/d\varepsilon$), for the chill, sand and high pressure die cast composites, plotted against true strain for tensile deformation. The differentiated loading curve for an unreinforced high pressure die cast AS41 sample is also shown in Figure 5d for comparison. With the composite materials none of the first derivatives of the loading curves show an obvious horizontal plateau at low strains, indicative of a purely elastic region. A similar effect was noted by Prangnell et al. in soft

aluminium matrix MMCs [5]. With the unreinforced die casting, the first derivative of the stress-strain curve (Figure 5d) does show a horizontal elastic plateau on initial loading, however, the slope in this region is below the published tensile stiffness of 45 GPa [15]. Nevertheless, the data clearly indicates that the highly clustered sand and chill cast composite materials exhibit no true pure elastic behaviour on tensile loading. For the HPDC composite material, which had a random particle distribution, there are some signs of a small linear portion of the stress-strain curve at very low applied stresses.

The absence of any pure-elastic region in the stress-strain curves of the composites on initial loading, except in the HPDC sample, is due to a combination of the presence of thermal residual stress in a soft magnesium matrix and stress concentration at the hard and angular SiC particles, leading to micro-yielding at a negligible applied load. A comparison of the tensile behaviours of the samples produced by the different casting routes indicates that, as has been previously postulated [5] the particle distribution has a significant effect on the development of plasticity and that highly clustered materials micro-yield at lower applied loads. This is presumably because greater local stresses are generated during loading in regions of higher local volume fraction and these regions would also be expected to have larger matrix thermal stresses, prior to loading. The other possible cause of the absence of a purely elastic region in the sand and chill cast samples is the growth of pre-existent casting defects, concentrated in the clustered regions, which could affect the stress-strain behaviours of these materials.

Investigation of the Fracture Behaviour

Examination on the fracture surfaces of all the composites suggest that they failed by a relatively brittle cleavage mechanism with only limited signs of localised plasticity. How the fracture path was affected by the local distribution of the reinforcement was investigated by the metallographic examination of cross-sections through the fracture surface. Figures 6 shows micrographs of cross-section of the fracture surfaces of the chill, sand and high pressure die cast composites after tensile testing at room temperature. The incidence of particle fracture, and the density of particles on and near the fracture surfaces, were analysed (see experimental section). Table 2 shows the result of the analysis averaged for both halves of three fractured samples for each material. The results show how significant localised particle concentration is to the fracture path. The local particle volume fractions measured within 200 μm of the fracture surface are very similar to the average bulk particle volume fractions, for all the materials. However the density of particles actually on the fracture surface are very different for the different casting processes (evaluated from the ratio of the total particle line length in the line of fracture to the fracture path length in the 2D section). The chill cast composite, that had the least ductility of ~ 0.5%, has the highest ratio of 0.43, over 3 times the average volume fraction. The sand cast material, which had a ductility of ~ 2% has a ratio of 0.36, and the HPDC material with the largest ductility and a nearly random particle distribution has a ratio of 0.12, which is similar to its bulk reinforcement volume fraction. In the case of the sand and chill cast materials, with the highly inhomogeneous particle distributions, the fracture path has clearly closely followed the regions of highest local particle volume fraction.

It is expected that as the matrix reinforcement bond strength increases, greater stress can be transferred to the particles prior to interface decohesion. If this stress in the particles is sufficiently large, particle cracking may occur prior to interface debonding. Because of the low instance of particle fracture observed in the materials investigated, fracture appears to occur by a combination of interfacial decohesion within the clustered particles, where large local hydrostatic stresses would be expected on loading, and by the crack path following non-wetted dry joints between clustered particles. The number of particles on the fracture surface of the die cast composite was much less than for the other two composite materials and this

was the only sample in which there were significant numbers of cracked particles (13 particles/mm^2) on and near the surface. This suggests that on average the particles experienced a greater stress during fracture in the HPDC material because with the random particle distribution the material was generally more resistant to crack propagation and there was also probably better wetting of the particles in the die casting process.

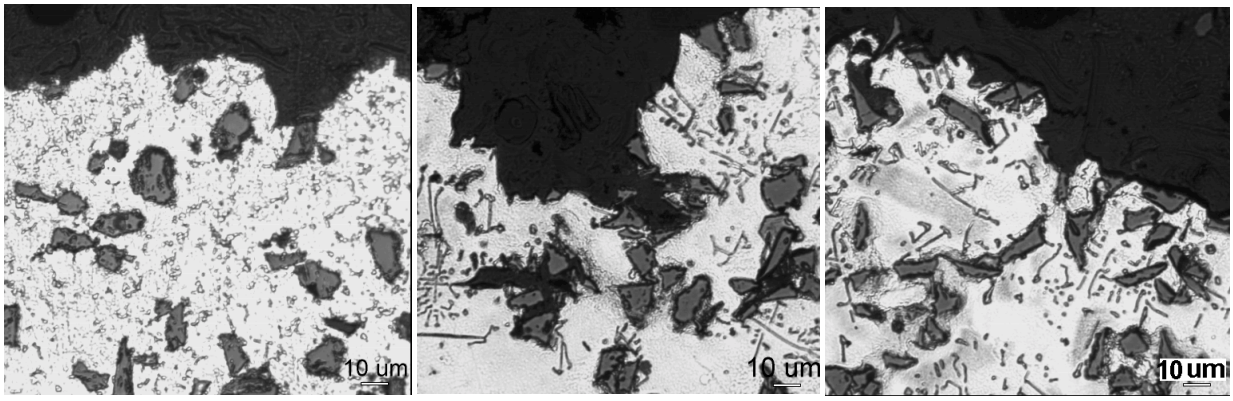

(a) (b) (c)

Fig. 6: Micrographs of cross-section of the fracture surfaces of the (a) high pressure die cast,(b) sand cast and (c) chill cast composites after tensile testing at room temperature.

Table 2: Particle density along the fracture line of the composites.

Materials	$\frac{\text{Particle length}}{\text{Fracture length}}$	Local particle volume fraction	No. of fractured particles/mm^2	Bulk particle volume fraction
Chill cast composite	0.43	0.12	0	0.13
Sand cast composite	0.36	0.12	9	0.15
HPDC composite	0.12	0.10	13	0.08

CONCLUSIONS

Quantitative analysis of the spatial distribution of the reinforcing particles has been used to interpret the tensile deformation and fracture behaviour of Mg alloy matrix composites cast by three different methods.

The bulk particle distributions were characterised using clustering parameters calculated from the statistical analysis of near-neighbour frequency distributions. The degree of clustering did not change systematically with cooling rate, but was most severe in the chill cast sample. In high pressure die casting, the particle distribution was virtually random because the cast grain structure developed on solidification was finer than the reinforcing particles. The tensile properties of the HPDC AS41 composite were generally far better than those of the sand and chill cast composites, due to the more homogeneous particle distribution and more refined matrix microstructure. The segregated distribution of SiC particles as well as the presence of other casting defects in particle clusters, like non-wetting, are thought to be responsible for the poorer properties of the chill and sand cast composites.

With the relatively soft matrix alloy investigated, it was found that neither of the sand or chill cast materials showed any pure elastic behaviour on initial loading, whereas the HPDC

material exhibited a very limited elastic plateau. This could be attributed to micro-plasticity occurring for a negligible applied stress, due to a combination of residual thermal stresses and stress concentration in the matrix, both of which would be expected to be greater in clustered regions of high local particle density.

All of the composites showed limited ductility, the strain to failure being strongly related to the degree of clustering determined by the clustering parameters. Analysis of the local particle distributions on the fracture surface showed that the fracture path followed the region of highest particle density and that 40% of the fracture length followed reinforcement interfaces in the most clustered casting.

ACKNOWLEDGEMENTS

M. Y. Ahmad is grateful to the Malaysian Government for financial support and the Authors are indebted to MEL for the provision of materials.

REFERENCES

1. T. W. Clyne, and P. J. Whiters, An Introduction to Metal Matrix Composites, 1993, Cambridge University Press,
2. W. H. Hunt Jr., O. Richmond, and R. D. Young, *ICCMVI & ECCMII* (Elsivier Applied Science Publishers Ltd. London, 1987), 2.209-2.223
3. N. Shi, B. Wilner, and R. J. Arsenault, *Acta metall. mater*., 1992,**39**,2481
4. D. L. McDanels, *Metal. Trans. A*, 1985,**16A**, 1105-1115
5. P. B. Prangnell, T. Downes, W. M. Stobbs and P. J. Withers, *Acta metall. mater.* 1994, **42**, 3425-3436
6. R. J. Arsenault, *Acta metall*., 1991,**39**, 1, 47-57
7. P. B. Prangnell, T. Downes, W. M. Stobbs and P. J. Withers, *Acta metall. mater.* 1994, **42**, 3437-3442
8. S. F. Corbin, and D. S. Wilkinson, *Acta metall. mater*., 1994, **42**, 1311-1318
9. R. J. Arsenault, N. Shi, C. R. Feng, and L. Wang, *Mater. Sci. Eng.*, 1991, A131, 55-68,
10. D. J. Lloyd, H. Lagace, A. McLeod, and P. L. Morris, *Mater. Sci. Eng.*, 1989, A107, 73-80
11. D. J. Lloyd, in *'Metal Matrix Composites - Processing, microstructure and properties', 12th Riso Inter. Symp. On Mat. Sci*.,1991, (ed. N. Hansen, et. al), Riso National Lab., 81-99
12. P. J. Wray, O. Richmond, and H. L. Morrison, *Metallography*, 1983, **16**, 39-58
13. I. C. Stone and P. Tsakiropoulos, *Mater. Sci. Tech*., 1995, **11**, 213-221
14. A.M. Murphy, S. J. Howard, and T. W. Clyne, Mater. Sci. Tech., 1998, **14**, 959-968
15. Elektron Database 2.1, 1994, *The Comprehensive Guide to Light Weight Mg alloys.* Magnesium Elektron and Eng. Info. Com: